eLIFE
elifesciences.org

RESEARCH ARTICLE

Figures and figure supplements

KLK3/PSA and cathepsin D activate VEGF-C and VEGF-D

Sawan Kumar Jha *et al*

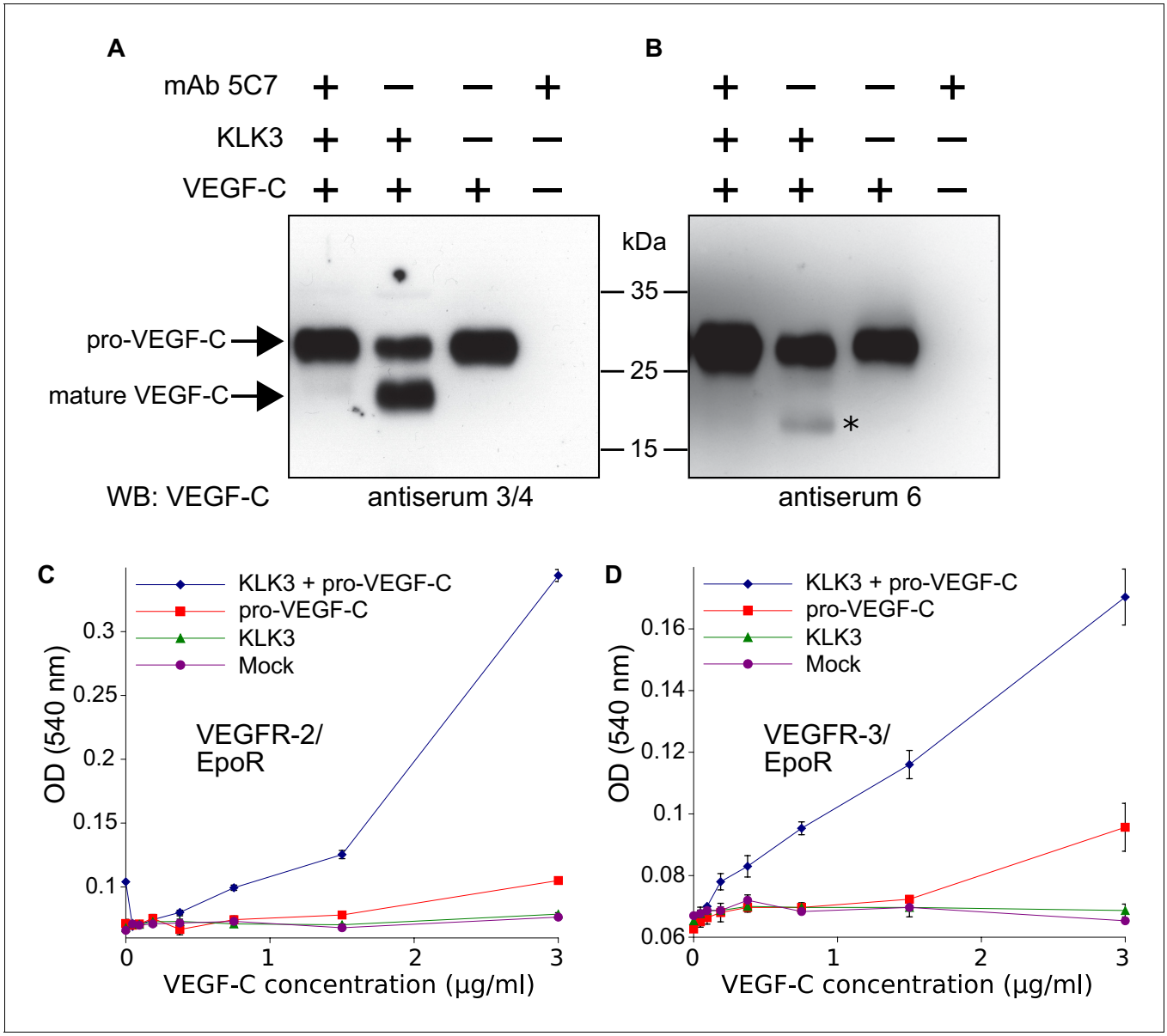

Figure 1. Kallikrein-related peptidase 3 (KLK3)/Prostate specific antigen (PSA) activates VEGF-C. (**A, B**) Cleavage of pro-VEGF-C by KLK3 (PSA). Pro-VEGF-C was incubated with or without KLK3, with and without the monoclonal antibody against KLK3 (5C7). Detection of VEGF-C in Western blots probed with antiserum 6 and 3/4, resulting in the detection of pro-VEGF-C (29/31 kDa) and activated, mature VEGF-C (21/23 kDa). The band marked by the asterisk likely represents the N-terminal propeptide (~15 kDa) which is detected by the antiserum 6. Note that for the image shown for antiserum 6, two different exposures of the same blot were merged (n = 3). (**C, D**) VEGF-C processed by KLK3 is biologically active in Ba/F3 cell assays, which translate activation of a hybrid VEGFR/EpoR receptor into cell survival (n = 2). Error bars indicate SD.

DOI: https://doi.org/10.7554/eLife.44478.003

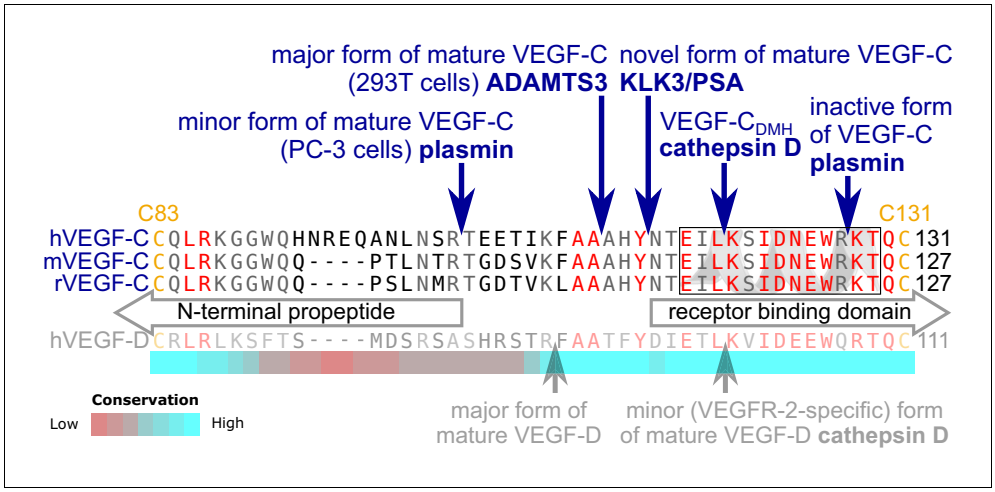

Figure 2. KLK3 activation of VEGF-C results in a unique VEGF-C species. KLK3 cleavage results in a mature VEGF-C species that is N-terminally three amino acids shorter than the ADAMTS3-cleaved VEGF-C. Shown are the aligned amino acid sequences between the N-terminal propeptide and the receptor binding domain of VEGF-C in human (h), mouse (m) and rat (r)VEGF-C and hVEGF-D. The arrows mark the sites of proteolytic cleavage of all four reported VEGF-C-activating enzymes and the two reported cleavage sites in VEGF-D. Residues within the N-terminal alpha-helix of VEGF-C/D are boxed. Note that the 1st plasmin cleavage site was not verified experimentally, but deduced from the plasmin cleavage signature and the size of the resulting product. The heat map under the alignment indicates the areas of highest divergence, deduced from a more comprehensive alignment of VEGF-C orthologs (see ***Figure 2—figure supplement 2***).

DOI: https://doi.org/10.7554/eLife.44478.005

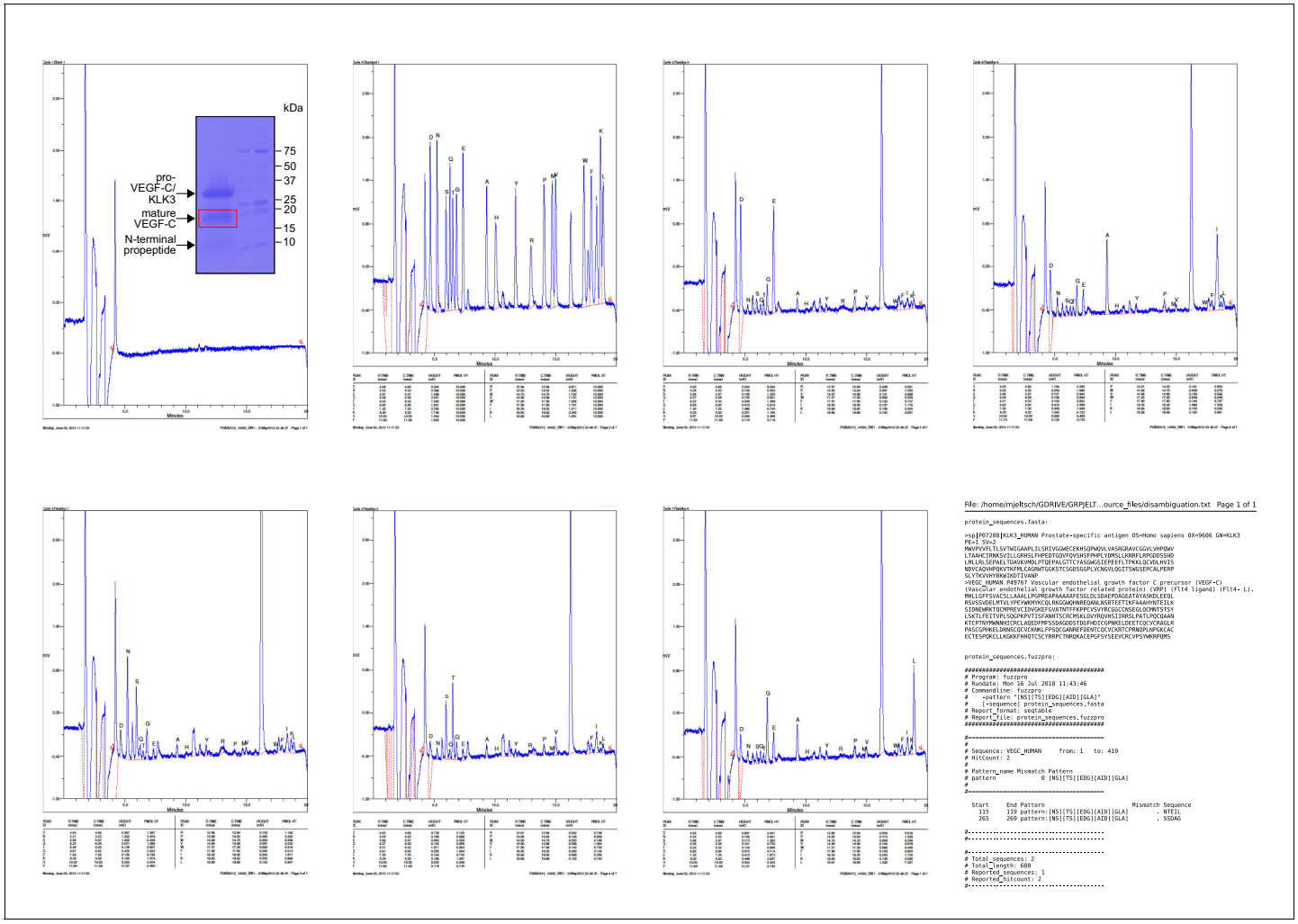

Figure 2—figure supplement 1. Results of the Edman degradation of KLK3-cleaved pro-VEGF-C. Because pro-VEGF-C contains already two N-termini due to the intracellular furin cleavage, fuzzpro was used to disambiguate three N-termini. Note that a third, minor KLK3 cleavage site was identified within the VEGF-C silk homology domain.

DOI: https://doi.org/10.7554/eLife.44478.006

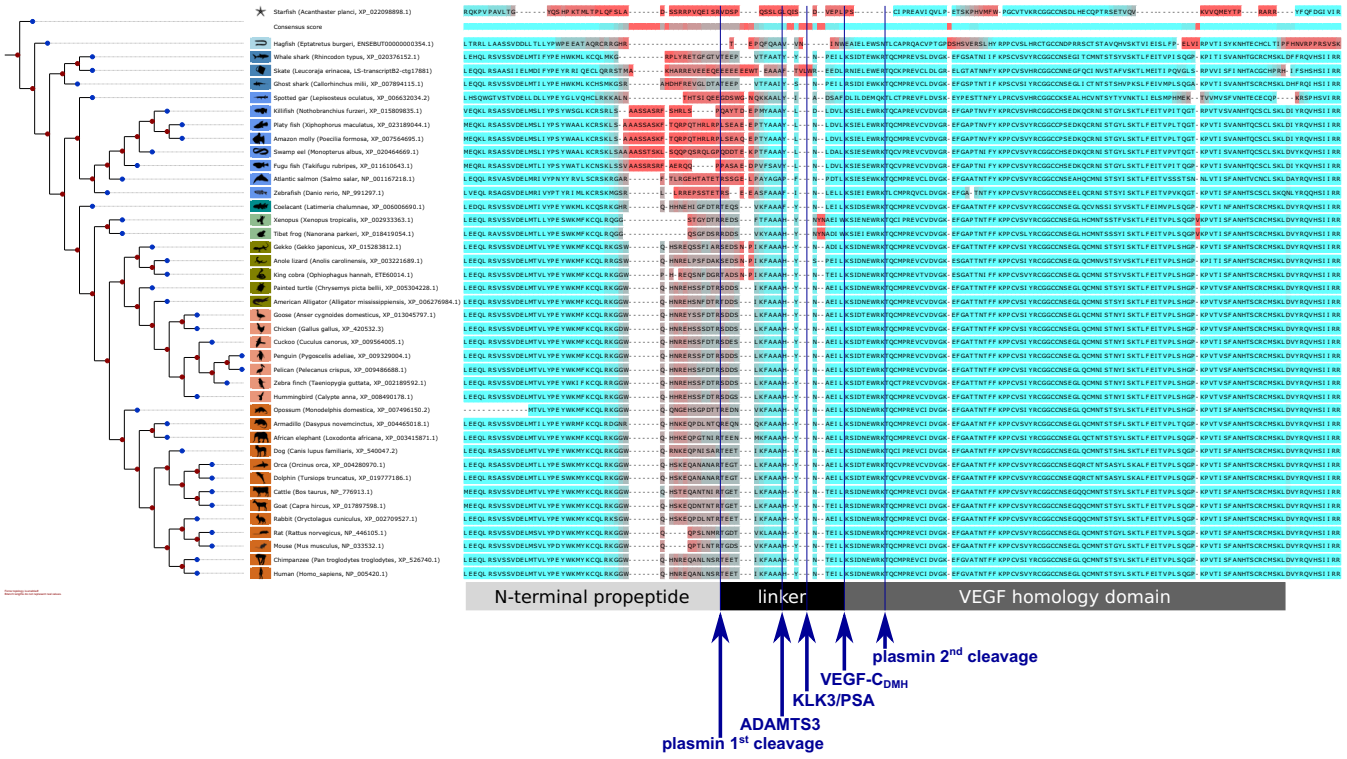

Figure 2—figure supplement 2. Interspecies analysis of VEGF-C amino acid sequences relevant for activation. While the VEGF homology domain (VHD) of VEGF-C is highly conserved among all vertebrates, the junction between the VHD and the N-terminal propeptide, which is important for the activation of VEGF-C, shows a significant divergence between different vertebrate clades, especially between most fish clades and the rest of the vertebrates. This divergence could be indicative of differences in the activation of VEGF-C. Note that the tree branches were set to a fixed length for better visual separation; therefore separation along the horizontal axis does not correspond to evolutionary distance. Amino acids were colored (red = high divergence, blue = high conservation) according to the Transitive Consistency Score (***Chang et al., 2014***). Complete parameters for the analysis can be retrieved from https://github.com/mjeltsch/VEGFC (***Jeltsch, 2018***).

DOI: https://doi.org/10.7554/eLife.44478.007

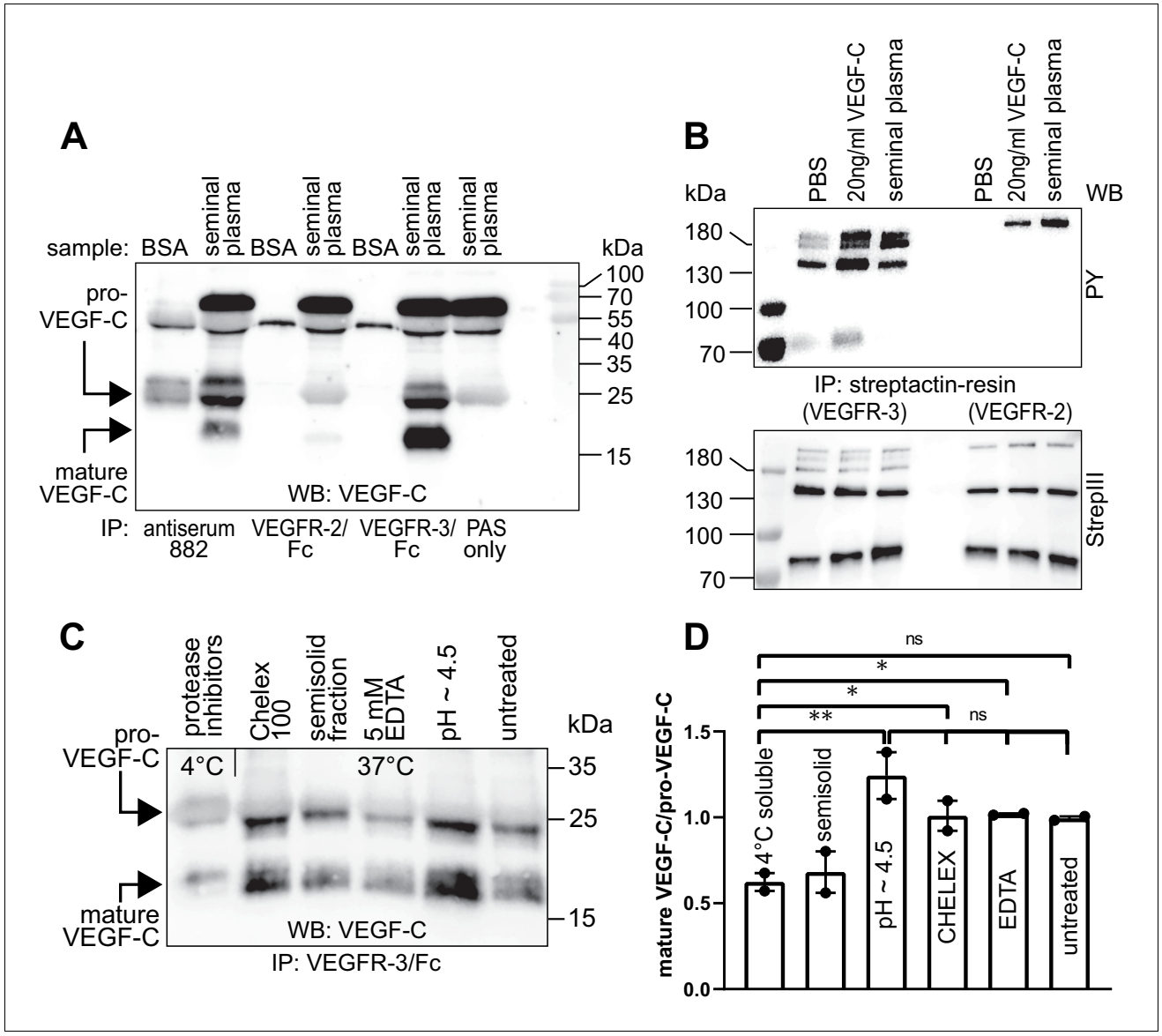

Figure 3. Seminal plasma VEGF-C is cleaved during sperm liquefaction and binds to and activates VEGFR-3. (**A**) Detection of both pro-VEGF-C and activated, mature VEGF-C by Western blotting with anti-VEGF-C antibody sc-374628 after pull-down with soluble VEGF receptors or antiserum 882. (**B**) Phosphorylation of VEGFR-2 and VEGFR-3 by seminal VEGF-C. Note that the phosphorylation pattern of VEGFR-3 is slightly different from that induced by 20 ng/ml of the VEGF-C control protein, which corresponds to the plasmin-activated form of VEGF-C. The lower panel shows the same blot reprobed with Streptactin-HRP for detection of the total levels of VEGFR-3 and VEGFR-2, respectively. (PAS, protein A sepharose; PY, phosphotyrosine) (**C**) Fresh seminal fluid contains less processed VEGF-C than seminal fluid liquefied at 37°C, indicating that pro-VEGF-C is converted into mature VEGF-C after ejaculation. Effect of protease inhibitors and low temperature on cleavage of VEGF-C (lane 1). While the mature VEGF-C/pro-VEGF-C ratios of ion sequestered samples (50 mg/ml CHELEX 100 and 5 mM EDTA in lanes 2 and 4, respectively) were not different from the untreated sample (lane 6), lowering the pH tended to increase the activation of VEGF-C (lane 5), but the difference to untreated sample did not reach statistical significance. Note that non-liquefied and liquefied samples differ because the semisolid seminogelins largely disappear during liquefaction (***Malm et al., 2000***). The semisolid fraction of fresh ejaculate was separately assessed for its VEGF-C content after liquefaction (lane 3). (**D**) Quantification of the ratio of mature VEGF-C to pro-VEGF-C in seminal plasma exposed to different conditions. Comparison of the 4°C sample to pH ~4.5 (p=0.0066), CHELEX (p=0.045), untreated (p=0.052), and EDTA (p=0.042) [One-way ANOVA, Dunnett's multiple comparisons test (n = 2), data are presented as mean ± SEM].

DOI: https://doi.org/10.7554/eLife.44478.008

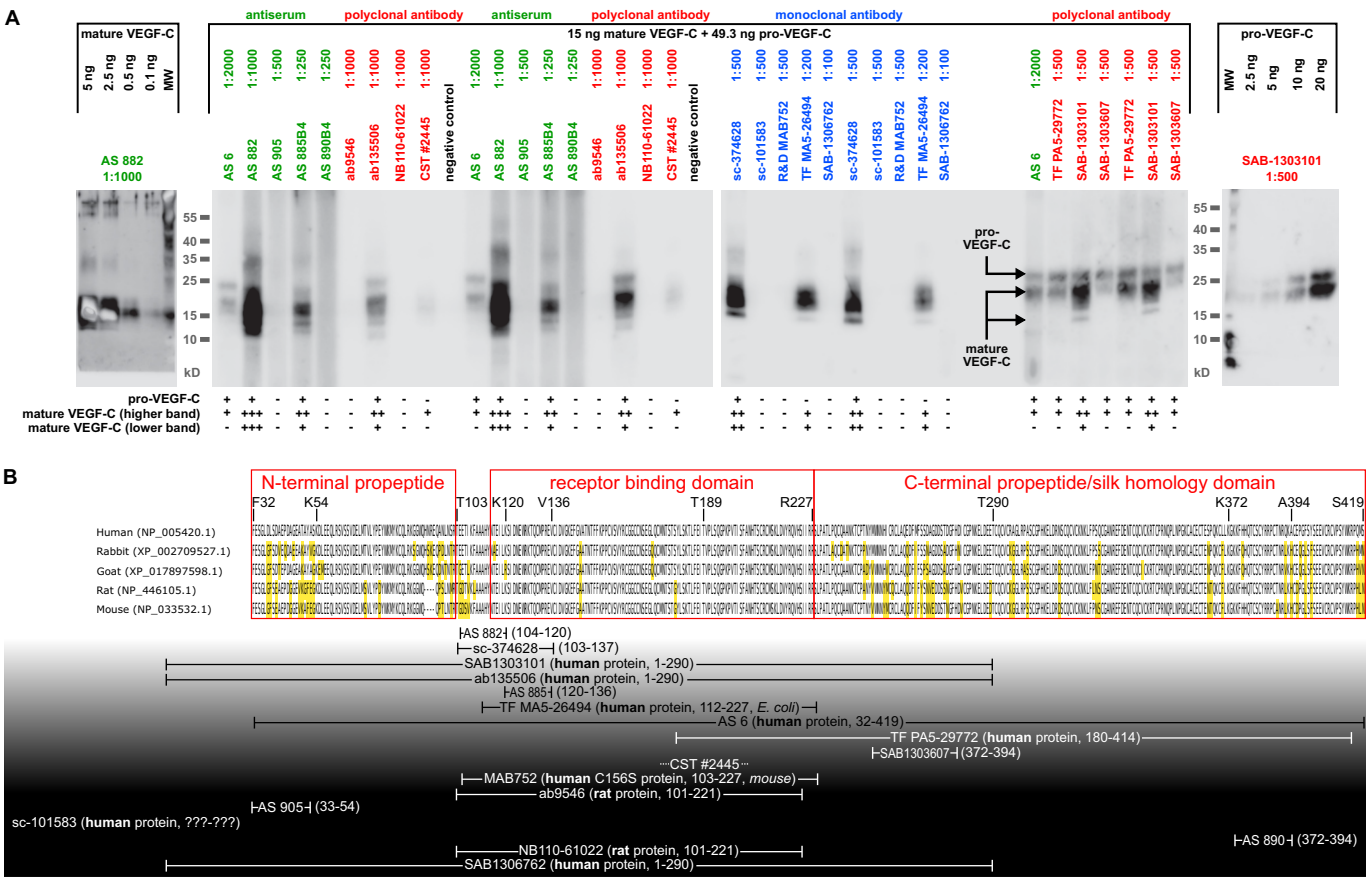

Figure 3—figure supplement 1. Comparison of 17 different antibodies for the detection of mature and pro-VEGF-C by Western blotting. (**A**) A mixture of equimolar amounts of mature VEGF-C and pro-VEGF-C was resolved on a single-well gel, and a miniblotter (MN20, Immunetics) was used to apply different primary and secondary antibodies during the detection procedure. Each individual slot corresponded to 15 ng of mature VEGF-C (***Kärpänen et al., 2006***) and 49.3 ng of pro-VEGF-C (***Jha et al., 2017***). Only 5 of the 17 antibodies recognized both pro-VEGF-C and both form VEGF-C, while eight antibodies recognized only the inactive pro-VEGF-C. seven antibodies failed completely to detect any VEGF-C form. Apart from sc-101583 (Santa Cruz Biotechnology), for which no detailed information was available about the antigen, all well-performing antibodies had been raised against a peptide or protein covering the junction between the N-terminal propeptide or the N-terminal end of the VEGF homology domain. However, since differently activated forms of VEGF-C feature different N-termini, the results of this screening are applicable only to the forms of VEGF-C used in this experiment: the minor (plasmin-generated) form of mature VEGF-C (***Joukov et al., 1996***) and pro-VEGF-C (also called 29/31-kDa-from) (***Joukov et al., 1997***). The unknown ratio between pro- and mature VEGF-C in a biological sample precludes the prediction of the net lymphangiogenic potential from an antibody-based VEGF-C signal from any of the antibodies that were tested. Antiserum (AS) no. six and monoclonal antibody sc-374628 proved to be in most cases sufficiently sensitive in detecting VEGF-C at physiologically relevant concentrations after immunoprecipitation. Although AS 882 showed a higher sensitivity compared to sc-374628, most experiments were performed with sc-374628 as it generated consistently lower background signal. (**B**) Peptides and proteins used for the immunization aligned to the VEGF-C amino acid sequences of relevant hosts. Antibodies are shown according to their signal strength from top (high sensitivity) to bottom (no detection). Amino acids differing from the human sequence are highlighted in yellow. All peptide antigens were derived from the human sequence. The amino acid residues covered by the antigens are given in brackets. For protein antigens, the sequence source species are indicated in bold and the expression host in italics if known. Note that the negative result of AS 905 is contrary to published data (***Joukov et al., 1997***) and might result from suboptimal antibody storage. AS 3/4 was not included in the comparison due to limited amounts available to us, and R and D Systems' AF752 was not included in the comparison since it was raised — differently from all other antibodies tested — in a goat host. The distinct capabilities to detect specific mature forms of VEGF-C is also seen in ***Figure 1***: AS no. 3/4 detects easily the mature KLK3-form of VEGF-C, whereas AS no.6 shows almost no signal. VEGF-C detection from any biological sample needs to take into account the interaction of pro-VEGF-C with extracellular matrix and cell surface proteins, which may introduce a bias into liquid samples. Similarly, active VEGF-C is a mobile species, potentially introducing a bias into solid samples as it can be lost during sample preparation. We determined typical seminal plasma VEGF-C levels by ELISA (R and D Systems' DVEC00) as being approximately 2.5 ng/ml VEGF-C (data not shown). However, these results are of limited value, since the calibration of the ELISA is performed using purified mature VEGF-C (minor form), whereas any biological sample will likely contain a mixture of pro-VEGF-C and different forms of mature VEGF-C.

DOI: https://doi.org/10.7554/eLife.44478.009

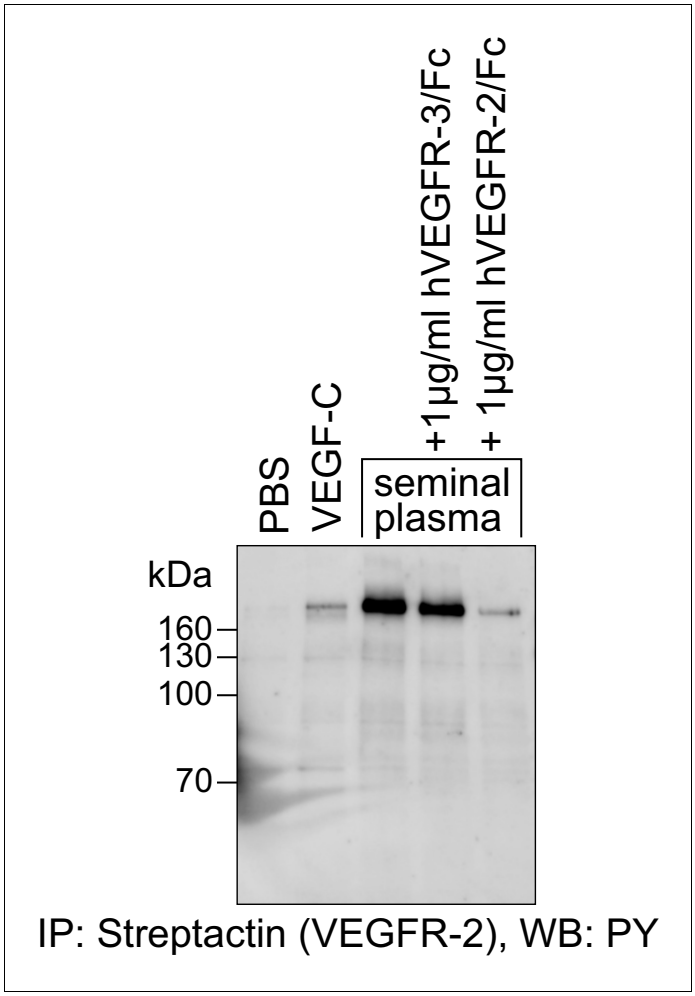

Figure 3—figure supplement 2. The VEGFR-2 phosphorylating activity of seminal plasma is blocked by the VEGF-A-capturing VEGFR-2/Fc fusion protein. Seminal plasma (diluted 1:1 with PBS) stimulated the phosphorylation of VEGFR-2 expressed in PAE cells. This stimulation was blocked efficiently by VEGFR-2/Fc fusion protein. VEGFR-3/Fc, which captures VEGF-C, but not VEGF-A, is inefficient in blocking the phosphorylation of VEGFR-2.

DOI: https://doi.org/10.7554/eLife.44478.010

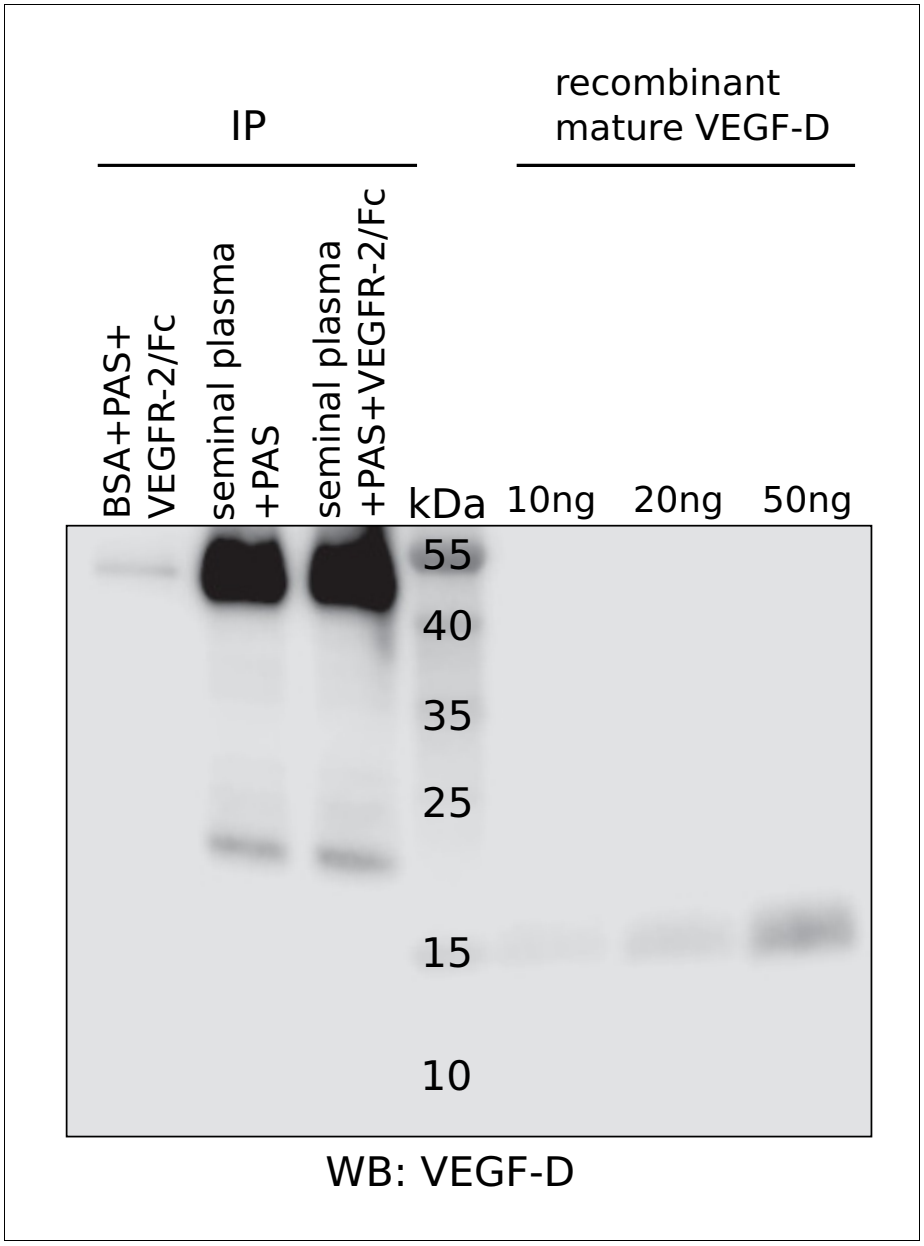

Figure 3—figure supplement 3. No detection of VEGF-D in seminal plasma. Liquefied seminal plasma was assayed for VEGF-D using R and D Systems' polyclonal anti-VEGF-D antibody after pull-down with VEGFR-2/IgGFc. VEGF-D was not detected. Unlike for VEGF-C, no extensive screening was performed to identify the antibody with the highest sensitivity and therefore, the presence of VEGF-D at low concentrations (<~10 ng/ml) cannot be excluded.

DOI: https://doi.org/10.7554/eLife.44478.011

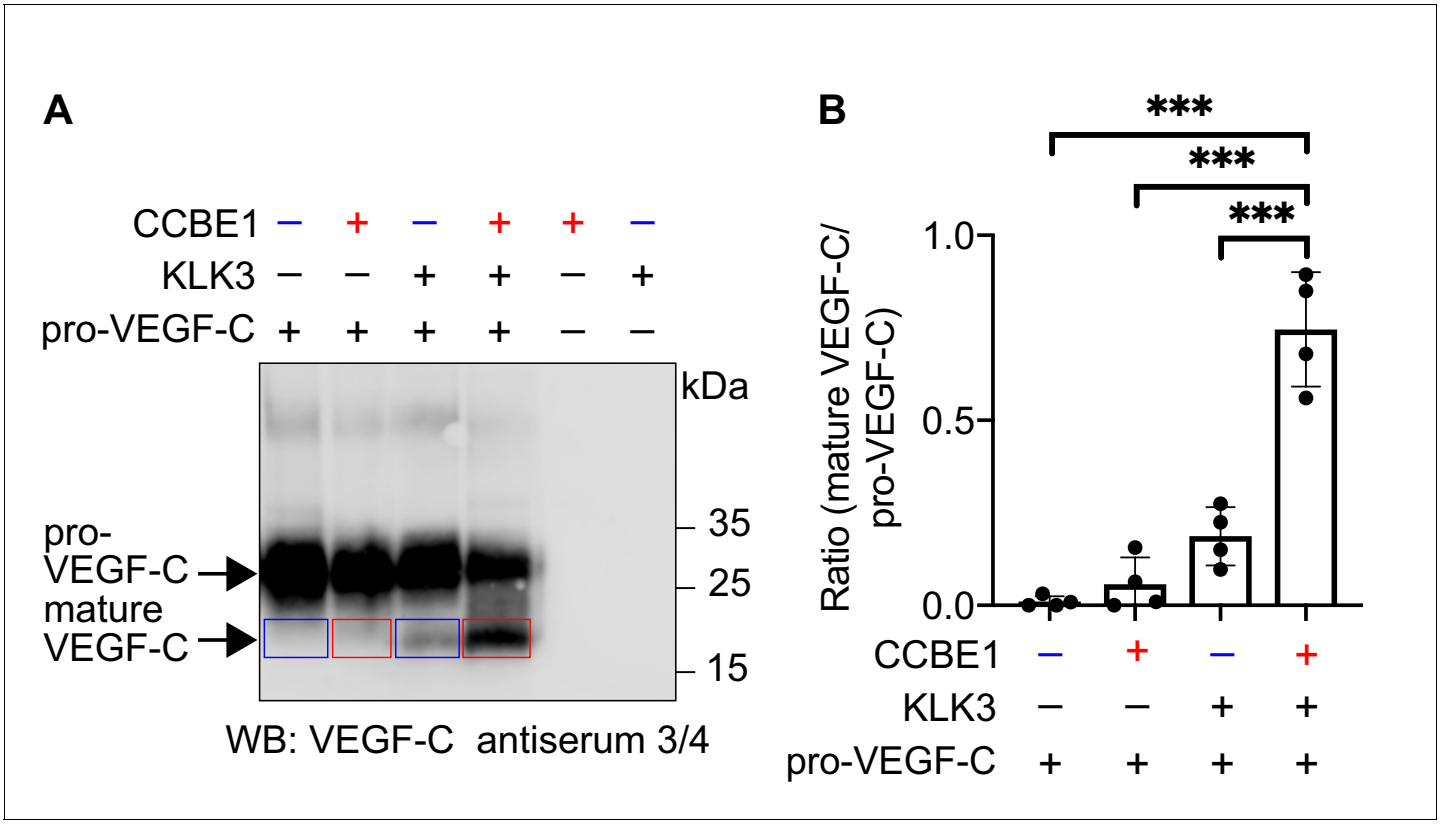

Figure 4. VEGF-C activation by KLK3 is enhanced by CCBE1. (**A**) Activation of VEGF-C by KLK3 is enhanced by CCBE1. The mature VEGF-C produced in the presence or absence of CCBE1 is shown in the red and blue boxes, respectively. (**B**) Quantification of the mature VEGF-C/pro-VEGF-C ratio. Data are shown as mean ± SD (n = 4). Statistical differences were determined by one-way ANOVA with Tukey *post hoc* test, ***p<0.001.

DOI: https://doi.org/10.7554/eLife.44478.013

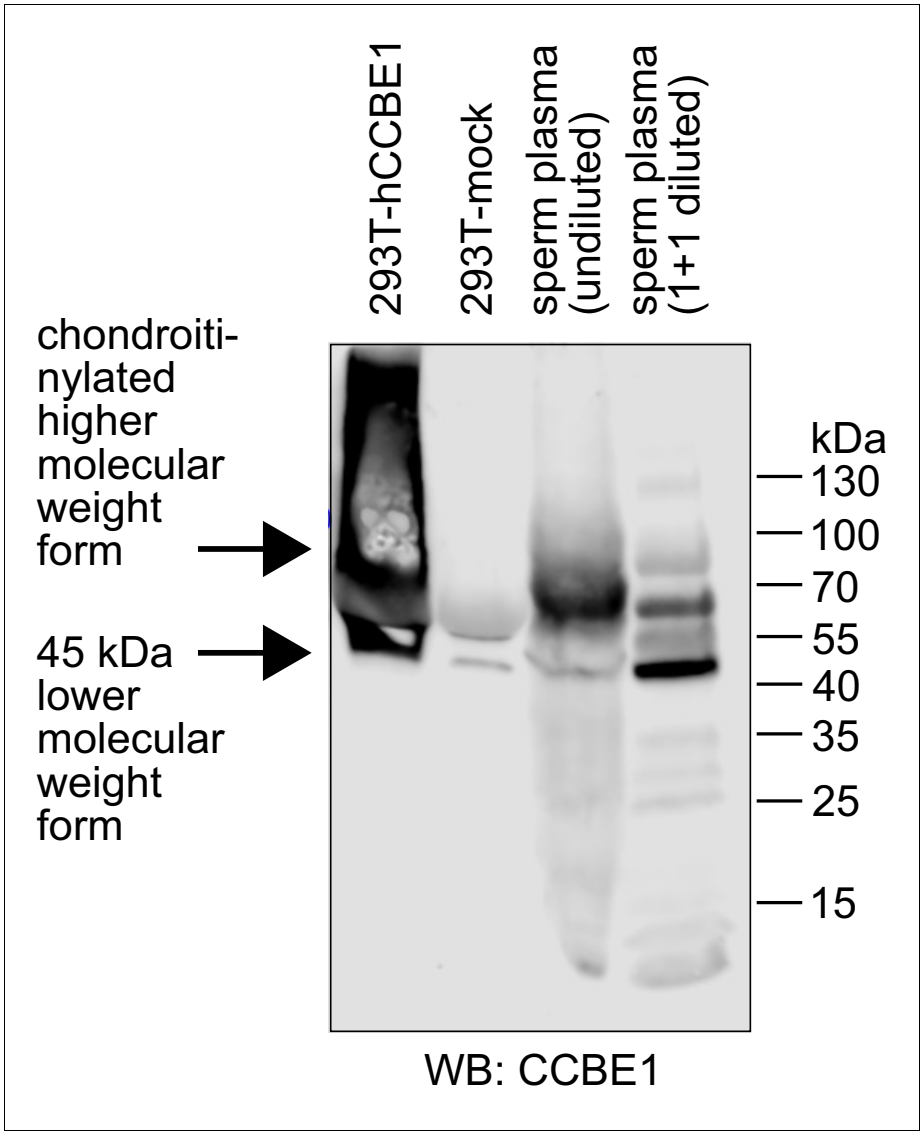

Figure 4—figure supplement 1. Seminal plasma contains CCBE1 protein. CCBE1 was detected by Western blotting in both diluted and undiluted seminal plasma samples. Supernatant from 293 T cells transfected with CCBE1 was used as a positive control. CCBE1 from 293 T cell supernatant presents as a distinct band of approximately 45–50 kDa and its chondroitinylated form as a smear of higher molecular weight (***Bui et al., 2016***; ***Jeltsch et al., 2014***). CCBE1 from seminal plasma shows the same lower-size band, but its higher molecular weight forms are more discrete compared to the 293T-produced product. While both seminal plasma CCBE1 and VEGF-C were readily detectable by Western blotting, we were not able to confirm the presence of VEGF-C in seminal plasma by protein mass spectrometry (data not shown). Similarly, a recent mass spec review of seminal proteins does neither identify VEGF-A nor VEGF-C (***Jodar et al., 2016***). We assume that this inability results from the combined effect of the very broad range of protein concentrations in seminal plasma and the fact that the highly abundant proteins in seminal plasma, like fibronectin and KLK3, are binding VEGF-C, which precludes their specific removal. Protein concentrations in seminal plasma range from values around and above 1 mg/ml for fibronectin (***Wennemuth et al., 1997***) and KLK3 (***Sensabaugh, 1978***) down to approximately 2.5 and 10 ng/ml for VEGF-C (this work) and the closely related growth factor VEGF-A (***Brown et al., 1995***), respectively.
DOI: https://doi.org/10.7554/eLife.44478.014

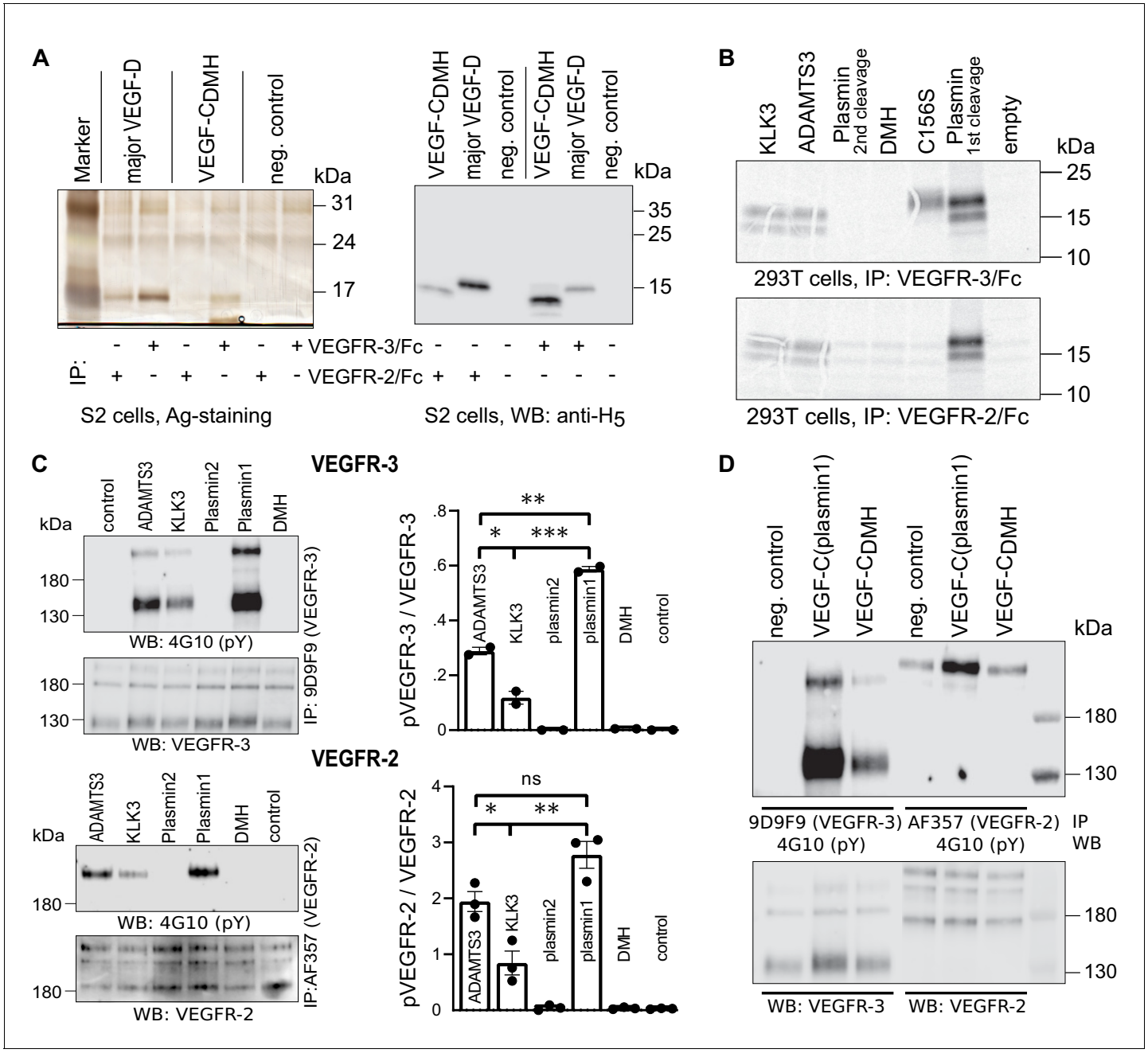

Figure 5. Shortening of the VEGF-C N-terminal helix reduces receptor binding and activation. (**A**) VEGF-C_{DMH} form binds efficiently to VEGFR-3 but weakly to VEGFR-2 when expressed in S2 cells. (**B**) Lack of binding of 293T-produced VEGF-C_{DMH} to VEGFR-2 or VEGFR-3. Note that the weak bands visible in the mock transfected 293T samples are due to endogenous VEGF-A, which binds to VEGFR-2, but not to VEGFR-3 (n = 2). (**C**) Stimulation of VEGFR-3 and VEGFR-2 phosphorylation by equimolar amounts of N-terminally truncated VEGF-Cs (corresponding to mature VEGF-C generated by ADAMTS3, KLK3, and the first plasmin cleavage) expressed in CHO cells (quantification: n = 2 for VEGFR-3; n = 3 for VEGFR-2; data are presented as mean ± SEM; one-way ANOVA, Tukey's multiple comparisons test). When compared with control, all three mature VEGF-C forms showed significant stimulation of both receptors (p-values=0.0094 to<0.0001). (**D**) Phosphorylation of hVEGFR-3 but not hVEGFR-2 in PAE cells by VEGF-C_{DMH} purified from S2 cells.

DOI: https://doi.org/10.7554/eLife.44478.016

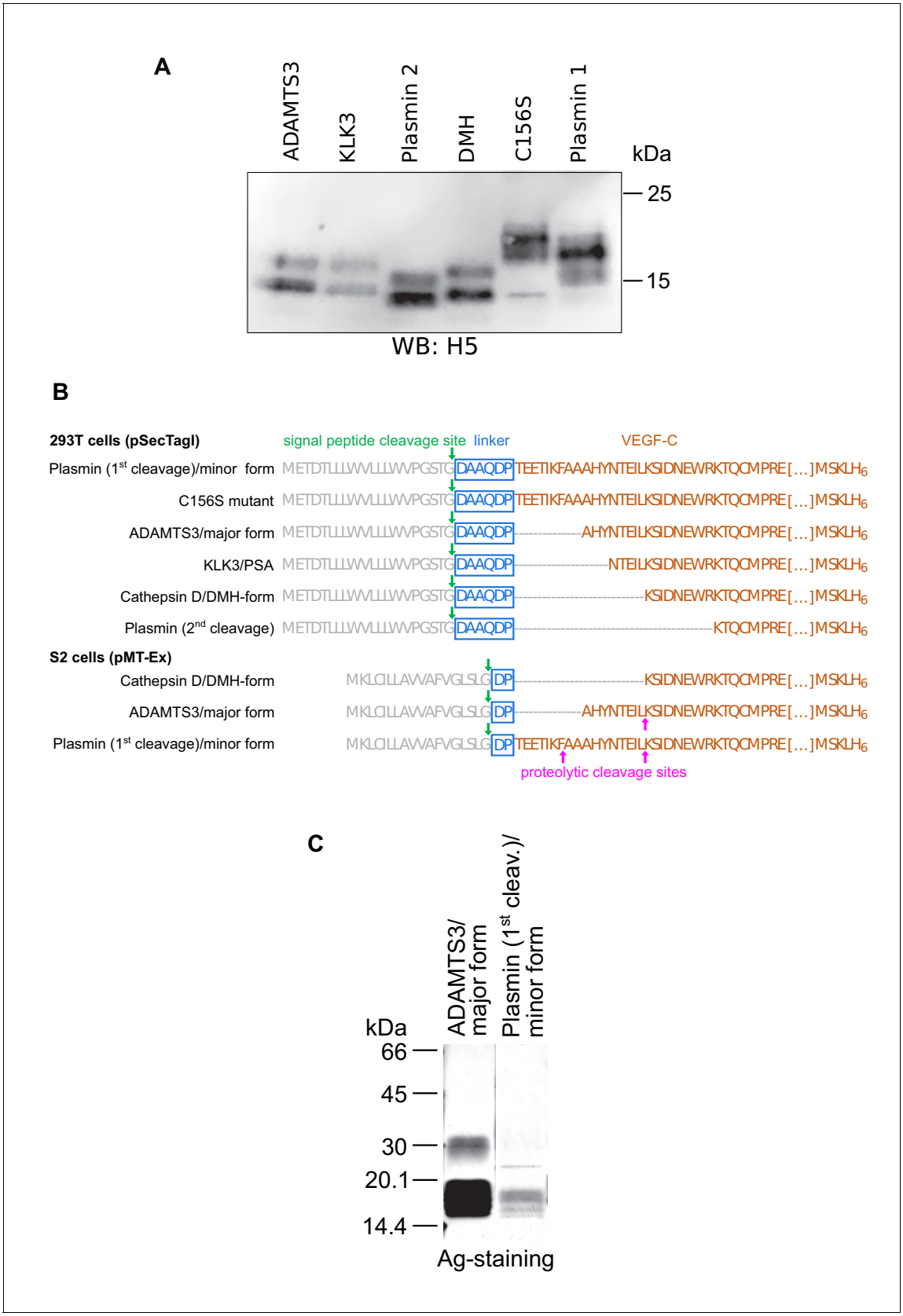

Figure 5—figure supplement 1. Secondary activation of a longer mature VEGF-C form in S2 cells. (**A**) Expression of N-terminally truncated VEGF-Cs in transiently transfected CHO cells. Equimolar amounts of VEGF-Cs were calculated based on a densitometric determination of VEGF-C concentrations

Figure 5—figure supplement 1 continued on next page

Figure 5—figure supplement 1 continued

from a Western blot of conditioned supernatant. (**B**) The N-terminally shortest active form of VEGF-C (DMH form) can be expressed from a truncated cDNA. The N-terminal propeptide was deleted to different extents from the VEGF-C cDNA resulting in the expression of mature VEGF-C forms corresponding to the enzymatic activation by different proteases. The C-terminal propeptide was deleted, and following Leu-215, a hexahistidine tag was added to enable comparative quantitation and purification. The cloning process leaves a 6-amino acid residue linker between the Ig Kappa signal peptide and the VEGF-C cDNA for the 293 T cell constructs but only a 2-amino acid residue linker between the BiP signal peptide and the VEGF-C cDNA for the S2 cell constructs. The longer linker of the mammalian DMH construct might be responsible for the inability of the 293T cell-produced VEGF-C_{DMH} to bind to VEGFR-2 and VEGFR-3 (this linker was removed for the generation of the corresponding adeno-associated virus, which induced lymphangiogenesis in skeletal muscle). (**C**) In S2 cells, the DMH-form of VEGF-C is generated via proteolytic processing from longer mature forms of VEGF-C (secondary activation). It was detected by N-terminal sequencing of VEGF-C produced by cells transfected with cDNA coding for the N-terminally longest, minor mature form (corresponding to the form generated by the 1 st plasmin cleavage). The secondary activation of minor mature form of VEGF-C was more efficient compared to the major mature form of VEGF-C (corresponding to the form generated by ADAMTS3 cleavage).

DOI: https://doi.org/10.7554/eLife.44478.017

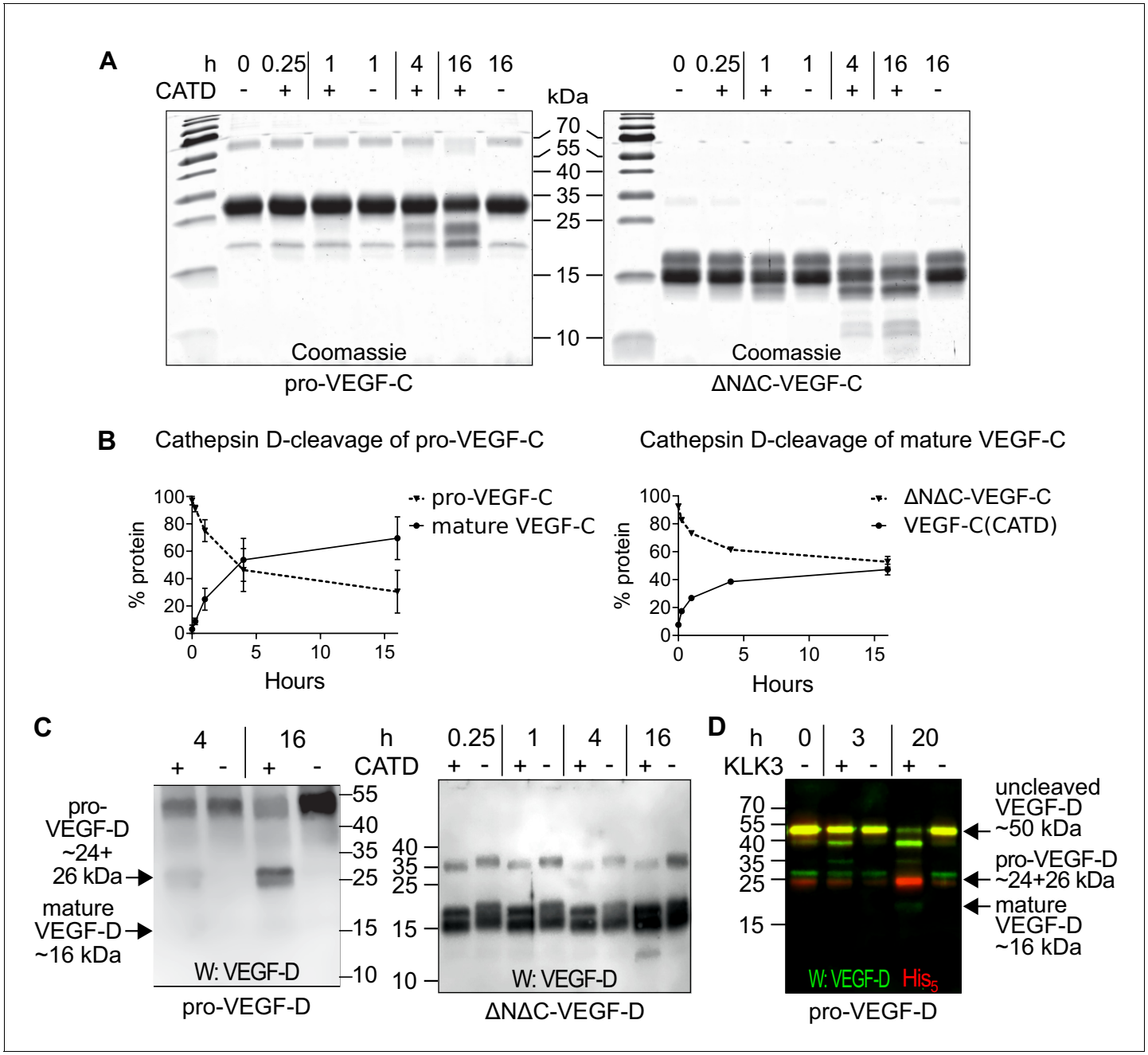

Figure 6. Cathepsin D activates pro-VEGF-C/D and mature VEGF-C/D, respectively. (**A**) Cleavage of VEGF-C by coincubation of pro-VEGF-C with cathepsin D (left panel) and secondary activation of ΔNΔC-VEGF-C (a mature form of VEGF-C translated from a truncated cDNA, right panel). (**B**) Quantification of the cleavage of pro-VEGF-C (n = 3) and ΔNΔC-VEGF-C (n = 2) by cathepsin D. (**C**) Cathepsin-D-mediated conversion of pro-VEGF-D into mature VEGF-D (left panel), and rapid activation of ΔNΔC-VEGF-D (a mature form of VEGF-D translated from a truncated cDNA, right panel). (**D**) Cleavage of pro-VEGF-D by KLK3. Note that, KLK3 cleaves VEGF-D between the VEGF homology domain and the N-terminal propeptide, but also between the VEGF homology domain and the C-terminal propeptide (for a detailed breakdown of the cleavage products visible in this overlay and the individual exposures, see ***Figure 7—figure supplement 2***) (n = 2).

DOI: https://doi.org/10.7554/eLife.44478.019

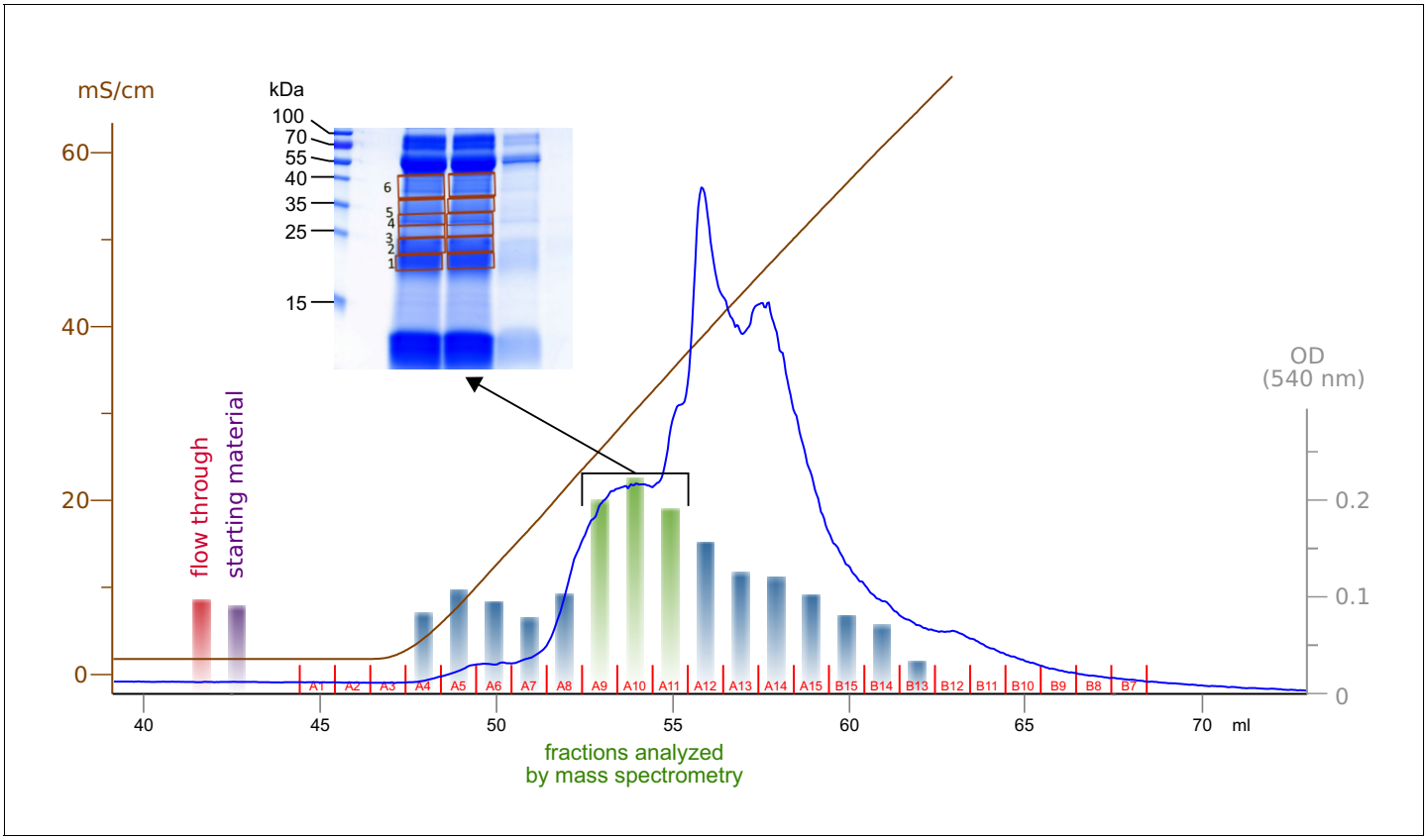

Figure 6—figure supplement 1. Enrichment and fractionation of VEGF-C cleaving activity. Sterile-filtered saliva was fractionated using cation exchange chromatography and fractions were analyzed by incubation with pro-VEGF-C, followed by assaying for active VEGF-C using BaF3/VEGFR-3 cells. The three fractions with the highest concentration of active VEGF-C were resolved by SDS-PAGE and six bands were excised for mass spectrometric analysis.

DOI: https://doi.org/10.7554/eLife.44478.020

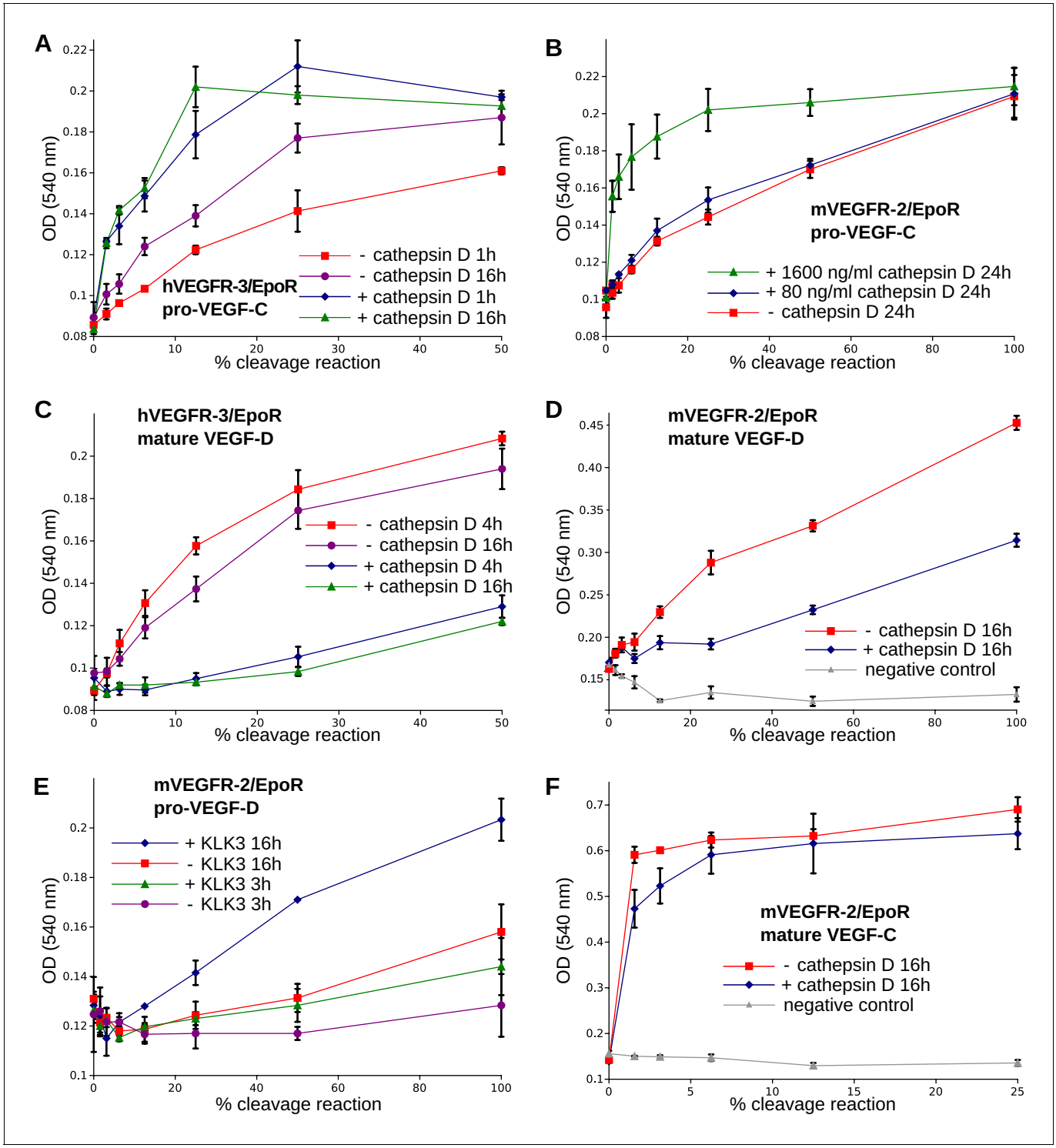

Figure 7. The receptor-activating properties of VEGF-C and VEGF-D are differentially affected by cathepsin D cleavage. Shown are the results of Ba/F3-VEGFR/EpoR assays used to evaluate the receptor-activating properties of cathepsin D- and KLK3- cleaved proteins. Cathepsin D-cleaved VEGF-C activity in the (**A**) Ba/F3-VEGFR-3/EpoR assay and (**B**) Ba/F3-VEGFR-2/EpoR assay. (**C**) Mature VEGF-D after secondary activation with cathepsin D in the Ba/F3-VEGFR-3/EpoR assay. (**D**) The minor form of mature VEGF-D generated by cathepsin D-cleavage is less active than the major mature form in the Ba/F3-VEGFR-2/EpoR assay. (**E**) KLK3 activation of VEGF-D increases its potency in the Ba/F3-VEGFR-2/EpoR assay. (**F**) The secondary activation of mature VEGF-C with cathepsin D led to a small decrease in the response of Ba/F3-VEGFR-2/EpoR cells (n = 2). Error bars indicate SD.

DOI: https://doi.org/10.7554/eLife.44478.022

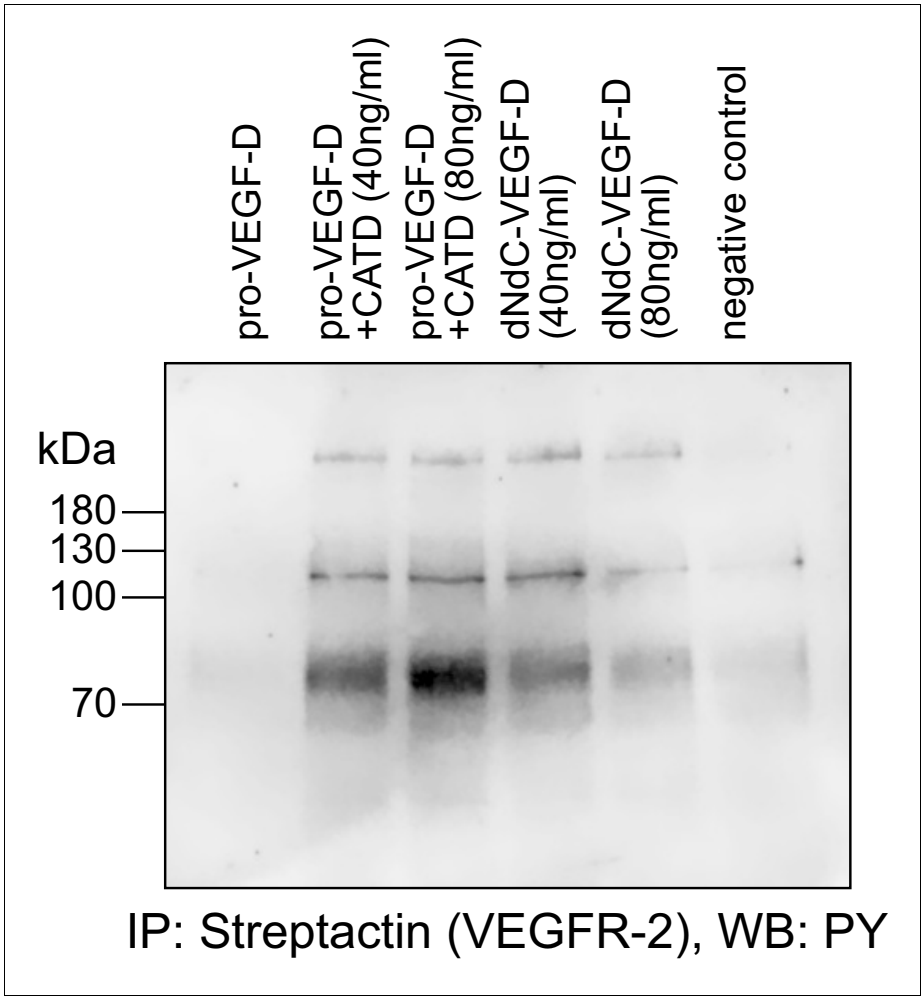

Figure 7—figure supplement 1. Cathepsin D-cleaved pro-VEGF-D stimulates the phosphorylation of VEGFR-2 in PAE cells. Pro-VEGF-D cleaved by cathepsin D stimulated the phosphorylation of VEGFR-2 expressed in PAE cells at 40 ng/ml and 80 ng/ml concentrations.

DOI: https://doi.org/10.7554/eLife.44478.023

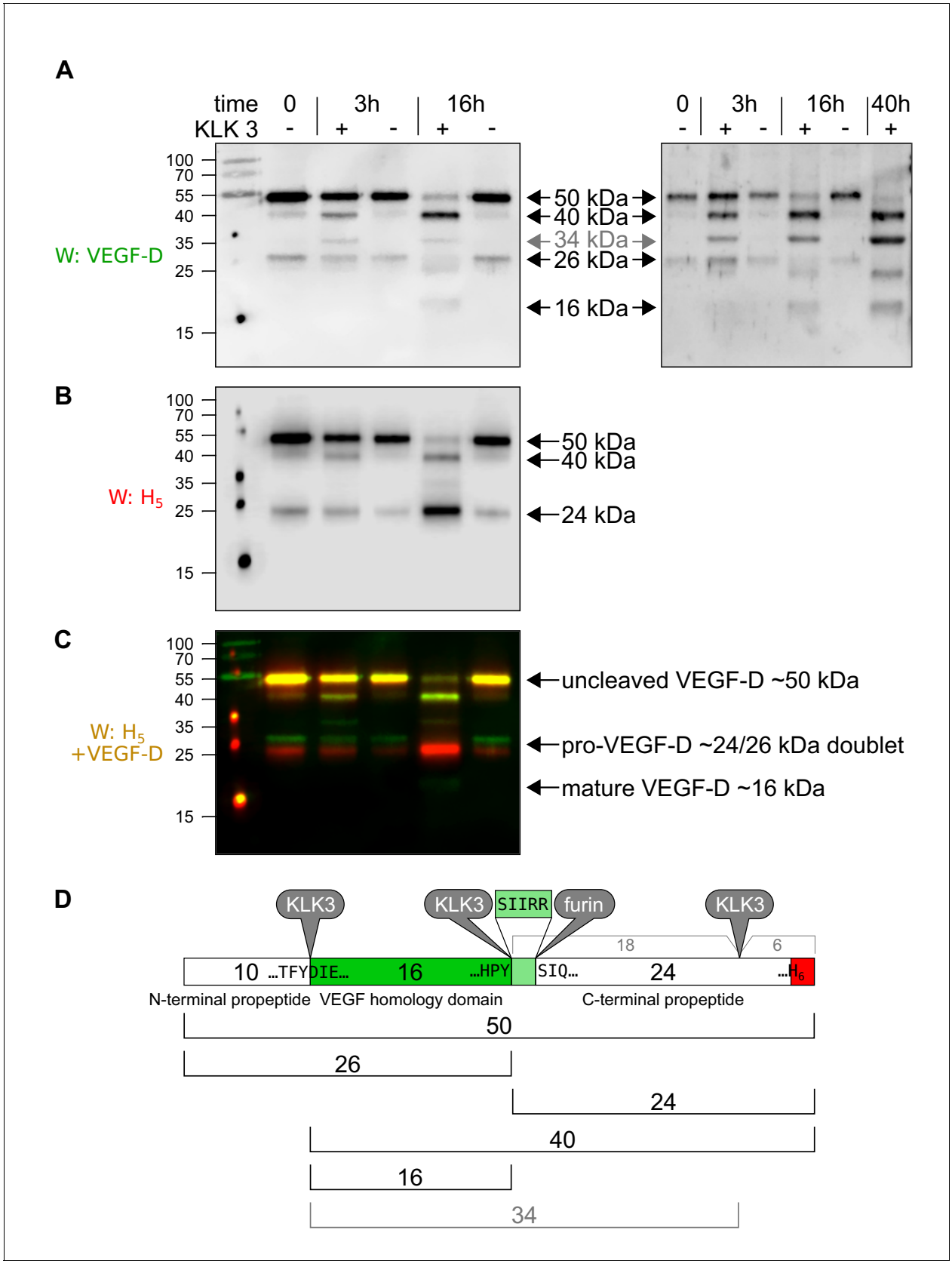

Figure 7—figure supplement 2. KLK3/PSA can proteolytically remove both propeptides from VEGF-D. When VEGF-D is overexpressed in the baculovirus system (**A–D**), CHO cells (data not shown) or 293 cells (***Stacker et al., 1999a***), a fraction of the protein does not become proteolytically

Figure 7—figure supplement 2 continued on next page

Figure 7—figure supplement 2 continued

processed beyond the cleavage of the signal peptide. Before KLK3 cleavage (time = 0), the VEGF-D produced in High Five cells consists of the uncleaved ~50 kDa form and a ~ 24/26 kDa doublet consisting of the C-terminal propeptide of ~24 kDa and its complement, the N-terminal propeptide and VEGF homology domain (VHD) of ~26 kDa. These sizes are about 5 kDa less compared to the 293-produced VEGF-D and the difference can be traced to the two glycosylation sites within the VHD, which contribute ~8 kDa in the 293 cells, but only ~3 kDa in HighFive cells. When co-incubated with KLK3, four cleavage products can be detected with an antibody specific for the VEGF homology domain (VHD; AF286, R and D Systems) (**A**), and two cleavage products can be detected with an antibody detecting the C-terminal hexahistidine tag (**B**). Based on the published proteolytic processing of VEGF-D (***Stacker et al., 1999a***), all cleavage products can be assigned based on their size and antibody reactivity to the known forms of VEGF-D (**D**). The unexpected 34 kDa band has previously been reported when VEGF-D is expressed in 293 cells and was attributed to an additional cleavage site near the C-terminus of C-terminal propeptide (***Stacker et al., 1999a***) and our data indicate that such cleavage occurs approximately 5 kDa before the end of the VEGF-D polypeptide between the third and forth C-X_{10}-C-X-C-$X_{1,3}$-C repeat. Based on the cleavage specificity of KLK3, the likely cleavage site between the VHD and the C-terminal propeptide is five amino acids shifted (to Tyr-200↓Ser-201) compared to the already described cleavage site (Arg-205↓Ser-206). Both the 34 and the 40 kDa bands disappear upon longer enzyme exposure (data not shown). KLK3-generated mature VEGF-D is not very well recognized by the VEGF-D antiserum, which is likely due to the fact, that the the antigen used to generate the polyclonal antibody against VEGF-D was produced from a truncated cDNA corresponding to the major mature form of VEGF-D, while the KLK3-generated form misses most of the highly immunogenic N-terminal amino acid residues from the major mature VEGF-D form.

DOI: https://doi.org/10.7554/eLife.44478.024

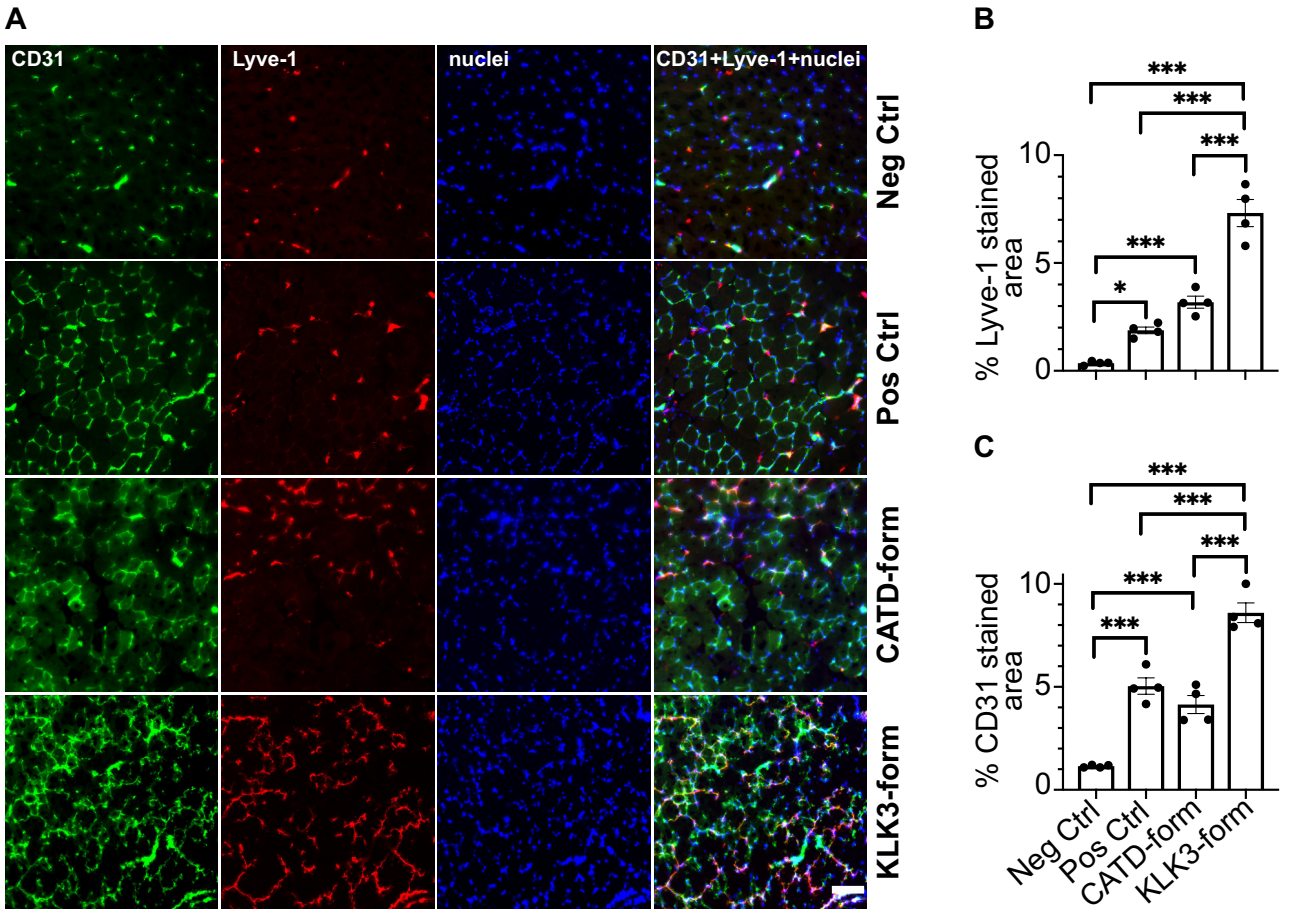

Figure 8. The KLK3- and cathepsin D-forms of VEGF-C induce lymphangiogenesis and angiogenesis in vivo. (**A**) Shown are the immunofluorescent stainings of the blood and lymphatic vessels in skeletal muscle transduced with recombinant adeno-associated virus subtype 9 (AAV9) encoding the KLK3- or the cathepsin D (CATD)-form of VEGF-C. Quantification of (**B**) Lyve-1 positive stained area and (**C**) CD31 positive stained area in AAV9 transduced tibialis anterior muscle. Data are presented as mean ± SEM, n = 4, one-way ANOVA with Tukey's *post hoc* test, ***p<0.001, *p<0.05. Scale bar, 100 µm. (see also ***Figure 8—figure supplement 1***).

DOI: https://doi.org/10.7554/eLife.44478.027

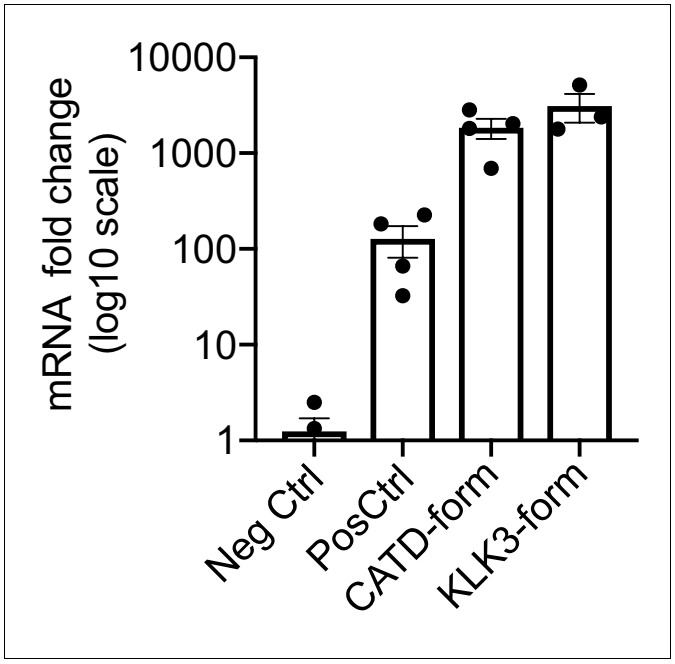

Figure 8—figure supplement 1. Expression of VEGF-C mRNA in tibialis anterior (TA) muscle. Comparison of VEGF-C mRNA levels in TA muscle transduced with AAV9 encoding for the different forms of mature VEGF-C generated by ADAMTS3 (Pos Ctrl), cathepsin D (CATD-form) and KLK3 (KLK3-form). Data are presented as mean ± SEM.

DOI: https://doi.org/10.7554/eLife.44478.028